Ballistic intracellular nanorheology reveals ROCK-hard cytoplasmic stiffening response to fluid flow

Jerry S. H. Lee[1,*], Porntula Panorchan[1], Christopher M. Hale[1], Shyam B. Khatau[1], Thomas P. Kole[1], Yiider Tseng[1,2] and Denis Wirtz[1,3,*]

[1]Department of Chemical and Biomolecular Engineering, The Johns Hopkins University, 3400 N. Charles St., Baltimore, MD 21218, USA
[2]Department of Chemical Engineering, University of Florida, Gainsville, FL 32011, USA
[3]Howard Hughes Medical Institute graduate training program, The Johns Hopkins University, 3400 N. Charles St., Baltimore, MD 21218, USA
*Authors for correspondence (e-mail: wirtz@jhu.edu; jslee@jhu.edu)

Accepted 19 January 2006
Journal of Cell Science 119, 1760-1768 Published by The Company of Biologists 2006
doi:10.1242/jcs.02899

Summary

Cells in vivo are constantly subjected to mechanical shear stresses that play important regulatory roles in various physiological and pathological processes. Cytoskeletal reorganizations that occur in response to shear flow have been studied extensively, but whether the cytoplasm of an adherent cell adapts its mechanical properties to respond to shear is largely unknown. Here we develop a new method where fluorescent nanoparticles are ballistically injected into the cells to probe, with high resolution, possible local viscoelastic changes in the cytoplasm of individual cells subjected to fluid flow. This new assay, ballistic intracellular nanorheology (BIN), reveals that shear flow induces a dramatic sustained 25-fold increase in cytoplasmic viscosity in serum-starved Swiss 3T3 fibroblasts. By contrast, cells stimulated with the actin contractile agonist LPA show highly transient stiffening of much lower amplitude, despite the formation of similar cytoskeletal structures. Shear-induced cytoplasmic stiffening is attenuated by inhibiting actomyosin interactions and is entirely eliminated by specific Rho-kinase (ROCK) inhibition. Together, these results show that biochemical and biophysical stimuli may elicit the formation of qualitatively similar cytoskeleton structures (i.e. stress fibers and focal adhesions), but induces quantitatively different micromechanical responses. Our results suggest that when an adherent cell is subjected to shear stresses, its first order of action is to prevent detachment from its substratum by greatly stiffening its cytoplasm through enhanced actin assembly and Rho-kinase mediated contractility.

Supplementary material available online at
http://jcs.biologists.org/cgi/content/full/119/9/1760/DC1

Key words: Cell mechanics, Rho GTPases, Fluid shear stress, Actin, Microtubule

Introduction

Fluid flows are necessary for proper cellular proliferation and growth, as well as the regulation of various physiological and pathological processes. Such fluid flow encompasses not only blood flow (Gimbrone, Jr, 1999), but also interstitial fluid flow that occurs through the extracellular matrix of tissues (Ng and Swartz, 2003). The cytoskeletal effects of hemodynamic forces on the vascular endothelium have been studied extensively. Endothelial cells adapt to shear flow by forming extended F-actin stress fibers that align in the direction of flow (Girard and Nerem, 1995; Langille et al., 1991; Malek and Izumo, 1996) and polarize by reorganizing the microtubule network to reposition the centrosome in the direction of flow (Tzima et al., 2003; Wojciak-Stothard and Ridley, 2003). Shear flows also cause changes in actin and microtubule structures in myofibroblasts and fibroblasts (Lee et al., 2005; Ng et al., 2005; Ng and Swartz, 2003; Poli et al., 2001), and influence their nuclear-receptor distributions and nucleus movement (Ji et al., 2003; Tseng et al., 2004). Reorganizations of cytoskeletal structures in endothelial cells and fibroblasts are coupled to the activity of members of the Rho GTPase family, including RhoA, Rac1 and Cdc42 (Hall, 1998; Nobes and Hall, 1995; Ridley and Hall, 1992; Ridley et al., 1992).

Fluorescence microscopy enables the visualization of the cytoskeleton architecture changes that take place in sheared cells, but cannot describe the micromechanical adaptations of the cytoplasm that occur in response to shear. Intracellular mechanics can depend on several factors – the extent of actin polymerization, actin filament organization, actomyosin contractility, and crosslinking and bundling of cytoskeleton filaments. Rheological investigations of reconstituted actin filament networks have long shown that subtle changes can have dramatic effects on the mechanical properties of actin networks, despite little to no change in actin architecture. Current cell mechanics methods are inadequate to probe the mechanical response of cells under shear. As the cells are encased in a chamber during shear stimulus, traditional extracellular methods of cell mechanics – e.g. AFM (Hoh and Schoenenberger, 1994), glass microneedles (Zheng et al., 1991), membrane-bound magnetic beads (Wang et al., 1993), micropipette suction (Evans et al., 1995), and microplate manipulation (Thoumine and Ott, 1997) – become unusable as they require a direct physical contact with the cell surface. In addition, fluid flow stresses acting on these probes are much larger than the adhesion forces between cell and probe, which

prevents real-time measurement of the mechanics of cells under shear.

To circumvent these limitations, we developed the method of ballistic intracellular nanorheology (BIN). The analysis of the random movements of microinjected fluorescent nanoparticles has been used previously to monitor changes in the micromechanical properties of the cytoplasm in cells subjected to biochemical stimuli (Kole et al., 2004a). Although effective, nanoparticle microinjection is inefficient and tedious. In addition, microinjection combined with nanoparticle tracking requires microscopy at high magnification; therefore, it would be difficult to locate the particle-injected cells after replating them for use in a flow chamber owing to the small population of injected cells. By using ballistic injection, rather than traditional microinjection, we are able to recover a much larger population of injected cells that can be readily located for visualization after being replated for use in the flow chamber.

We report here that the application of shear to serum-starved Swiss 3T3 fibroblasts induces a remarkable 25-fold increase in cytoplasmic viscosity and a 4-fold increase in elasticity. Pretreatment with an actomyosin interaction inhibitor attenuates this cytoplasmic stiffening phenomenon, whereas a specific Rho-kinase (ROCK) inhibitor completely eliminates shear-induced cell stiffening. These results suggest that a cell under shear flow maintains its adhesion to the underlying substratum by adapting the physical properties of its cytoplasm via the Rho-kinase-mediated pathway.

Results

Shear flow induces cytoskeleton stiffening in Swiss 3T3 fibroblasts

To investigate whether cells adapt the mechanical properties of their cytoplasm in response to shear flows, we subjected serum-starved Swiss 3T3 fibroblasts to fluid flow (shear stress, 9.4 dyn/cm^2). Serum-starvation of fibroblasts eliminates polarity responses during wound healing (Palazzo et al., 2001) and retards microtubule dynamics (Danowski, 1998), which we hypothesized would allow us to focus primarily on F-actin response to shear stimulus. To test this hypothesis, serum-starved cells were subjected to shear flow and a polarity assay was applied. Compared with serum-treated cells, shear flow did not induce changes in polarity in serum-starved fibroblasts (Fig. S1 in supplementary material). By contrast, immunofluorescence microscopy revealed that fluid shear stress stimulated actin assembly and the formation of actin stress fibers terminated by vinculin-containing focal adhesions in serum-starved fibroblasts (Fig. 2A, right inset). Unsheared serum-starved cells exhibited an actin-rich rim at the cell periphery and few actin stress fibers (Fig. 2A, left). This outcome allowed us to primarily focus on changes in intracellular mechanics resulting from shear-induced actin cytoskeleton reorganization and actomyosin contractility.

To assess the mechanical response of the cytoskeleton of cells under shear, we used particle tracking coupled to a new high-throughput injection modality (Fig. 1A). Cells were first ballistically injected with 100-nm fluorescent nanoparticles, then serum-starved for 48 hours, and finally subjected to external fluid shear stress. Ballistic injection, rather than traditional manual microinjection, allowed us to probe a large number of individual cells. The motion of individual ballistically injected nanoparticles embedded in the cytoplasm of sheared and unsheared cells was tracked, one cell at a time, with 10-nm spatial resolution and 33-millisecond temporal resolution using video-enhanced time-resolved fluorescence microscopy and a multiple-particle tracking software. The extent of the displacements of the nanoparticles reflects the local viscoelastic properties of the cytoplasmic milieu surrounding each nanoparticle (see more details in Materials and Methods). The motion of nanoparticles in a viscous liquid is diffusive and becomes sub-diffusive in a viscoelastic material.

The extent of movement of the nanoparticles in the cytoplasm of sheared cells was significantly smaller (Fig. 1B,

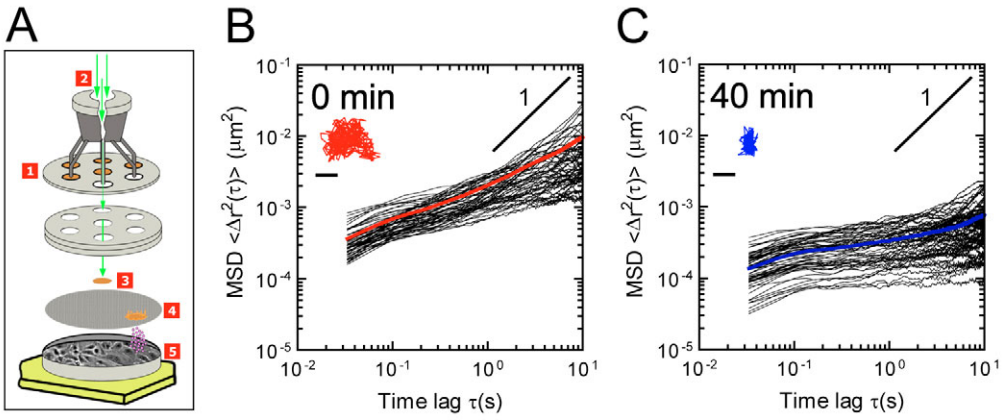

Fig. 1. Ballistic injection and tracking of nanoparticles embedded in the cytoplasm of adherent cells. (A) Schematic of the method of ballistic injection used to efficiently transfer nanoparticles to the cytoplasm of adherent cells. (1) Macrocarriers coated with 100 nm fluorescent nanoparticles are placed into a hepta adapter. (2) Pressurized helium gas (~2200 psi) flows through the adapter, and (3) accelerate the macrocarriers toward a stopping screen. (4) Macrocarriers are stopped by the screen and (5) nanoparticles cross the plasma membrane and penetrate the cytoplasm of adherent cells. Typical mean squared displacements (MSD) of nanoparticles in unsheared (B) and sheared (C) serum-starved Swiss 3T3 fibroblasts. Ensemble average MSD is overlaid for unsheared (red) and sheared (blue) fibroblasts. The insets show typical trajectories of the centroids of nanoparticles imbedded in the cytoplasm of cells before (B) and after (C) the application of 40 minutes of shear flow (shear stress, 9.4 dyn/cm^2). Bars in insets, 50 nm.

inset) than in unsheared cells (Fig. 1C, Inset). Analysis of the mean-squared displacements (MSDs) (Fig. 1B) showed that injected nanoparticles underwent random motion and showed no directed motion. Such behavior is expected from the forced injection of nanoparticles into the cytoplasm, which circumvents endocytosis, as opposed to passive uptake of the nanoparticles by the cells. Nanoparticles in both sheared and unsheared cells underwent unbiased random motion in the cytoplasm, as their MSD grew as a function of time with a slope equal to, or lower than, 1, $\langle \Delta r^2(\tau) \rangle \sim \tau^{\alpha}$ with $\alpha \leqslant 1$ (Fig. 1B,C). Nanoparticles undergoing activated motion within the cytoplasm would display an MSD growing faster than time, $\langle \Delta r^2(\tau) \rangle \sim \tau^{\alpha}$ with $\alpha > 1$, which was never observed. The same nanoparticles passively engulfed in the cytoplasm undergo directed motion (data not shown), which would prevent the use of endocytosis as a method of transfer of nanoparticles to the cytoplasm to probe its micromechanical properties.

The MSDs of the ballistically injected nanoparticles were mathematically transformed into parameters that described rigorously the mechanical properties of the cytoplasm, including its shear viscosity, elasticity, and shear compliance (see definitions of these terms for the non-specialist in Materials and Methods). This analysis showed that the cytoplasm of fibroblasts responded to shear flow by becoming significantly stiffer (i.e. more elastic) and more viscous. Fig. 2A illustrates the phenomenon of stiffening of the cytoplasm in cells under shear flow. Nanoparticles were color-coded according to the local compliance of the cytoplasm measured by the extent of the random displacements of the nanoparticles over 20 seconds: blue for stiffer regions, red for softer regions. We found that fluid flows induced a remarkable ~25-fold increase in cytoplasmic viscosity and a ~4-fold increase in its elasticity (Fig. 2B,C). The decrease in the slope of the shear compliance (Fig. 2B) also indicated that the cytoplasm of sheared cells became significantly more solid-like than that the cytoplasm of unsheared cells. The shear-enhanced difference between elastic and viscous moduli, G' and G'' (Fig. 2B), showed that the cytoplasm of sheared cells became more solid-like than that of unsheared cells, as indicated by a significantly lower phase angle, $\delta = \tan^{-1}(G''/G')$ (Fig. 2D).

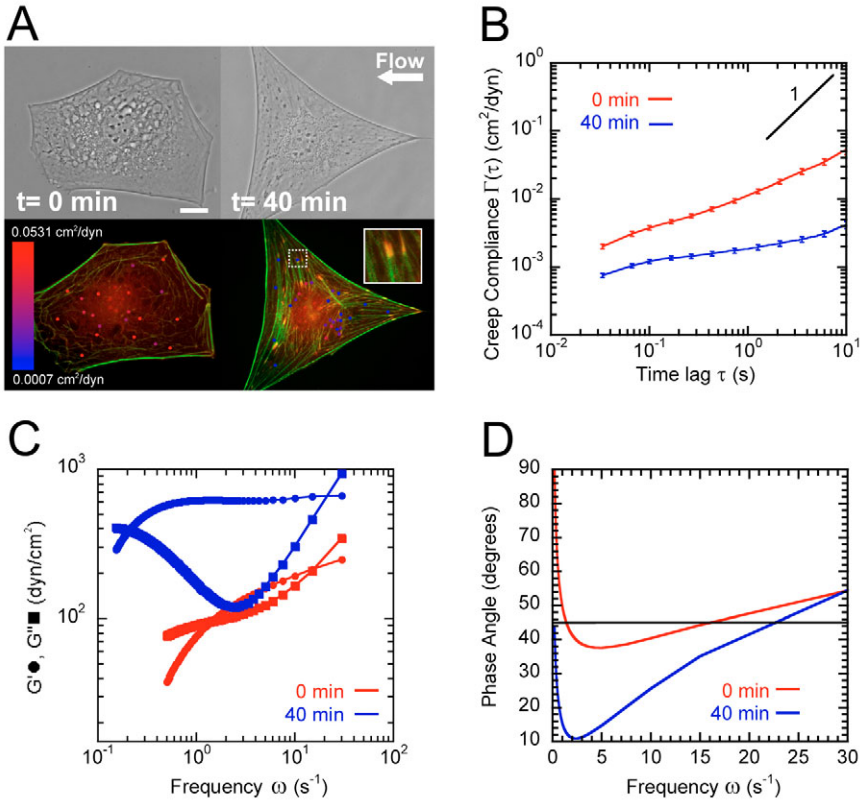

Fig. 2. Micromechanical response of serum-starved cells to shear flow. (A) Phase-contrast (top) and immunofluorescence (bottom) micrographs of Swiss 3T3 fibroblasts before (left) and after (right) shear flow. Actin (green) and vinculin (red) structures were overlaid with a micrograph of injected nanoparticles, which were colored according to the local value of the cytoplasmic deformability (evaluated at time scale of 0.1 seconds). The nanoparticles were enlarged to aid visualization. Blue denotes the least deformable (stiffest) regions of the cytoplasm; red denotes the most deformable (softest) regions. The inset is a magnified view of focal adhesions at the ends of actin stress fibers. Bar, 20 μm. (B) Shear compliances (i.e. deformability) of the cytoplasm of Swiss 3T3 fibroblasts before (red) and after 40 minutes of shear flow (blue) (n=6). Values represent mean ± s.e.m. (C) Frequency-dependent viscous and elastic moduli of cytoplasm, $G'(\omega)$ (circles) and $G''(\omega)$ (squares). (D) Frequency-dependent phase angle of cytoplasm, $\delta(\omega) = \tan^{-1}(G''/G')$, calculated from viscoelastic moduli shown in panel C. From a rheological standpoint, a phase angle of 90° describes the rheological behavior of a liquid; a phase angle of 0° describes the rheological behavior of a stiff solid.

Inhibition of actomyosin interactions diminishes shear-induced cytoplasmic stiffening

Given the formation of focal adhesions and stress fibers in sheared cells, we hypothesized that actomyosin contractility played a key role in the mechanical response of the cytoplasm of cells subjected to shear flows. We first tested whether weakened actomyosin interactions would affect the phenomenon of shear-induced cytoplasmic stiffening via pretreatment of cells with 2,3-butanedione 2-monoxime (BDM) for 30 minutes. BDM weakens actomyosin interactions by decreasing the ATPase activity of non-muscle myosin II (Fenteany and Zhu, 2003; McKillop et al., 1994) but does not significantly affect actin assembly (Riveline et al., 2001; Wojciak-Stothard et al., 1998; Zhong et al., 1998). In the absence of shear, BDM treatment alone did not significantly affect cell morphology and the level of cytoplasmic viscoelasticity (Fig. 3A, n=3). In the presence of shear, the cytoplasmic viscosity of BDM-treated cells increased only slightly (Fig. 3B, n=4) when compared with BDM-treated unsheared fibroblasts. These results confirm that actomyosin interactions are necessary for shear-induced cellular stiffening phenomenon and that the inhibition of such interactions, but not actin reorganization, attenuates shear-induced cytoplasmic stiffening.

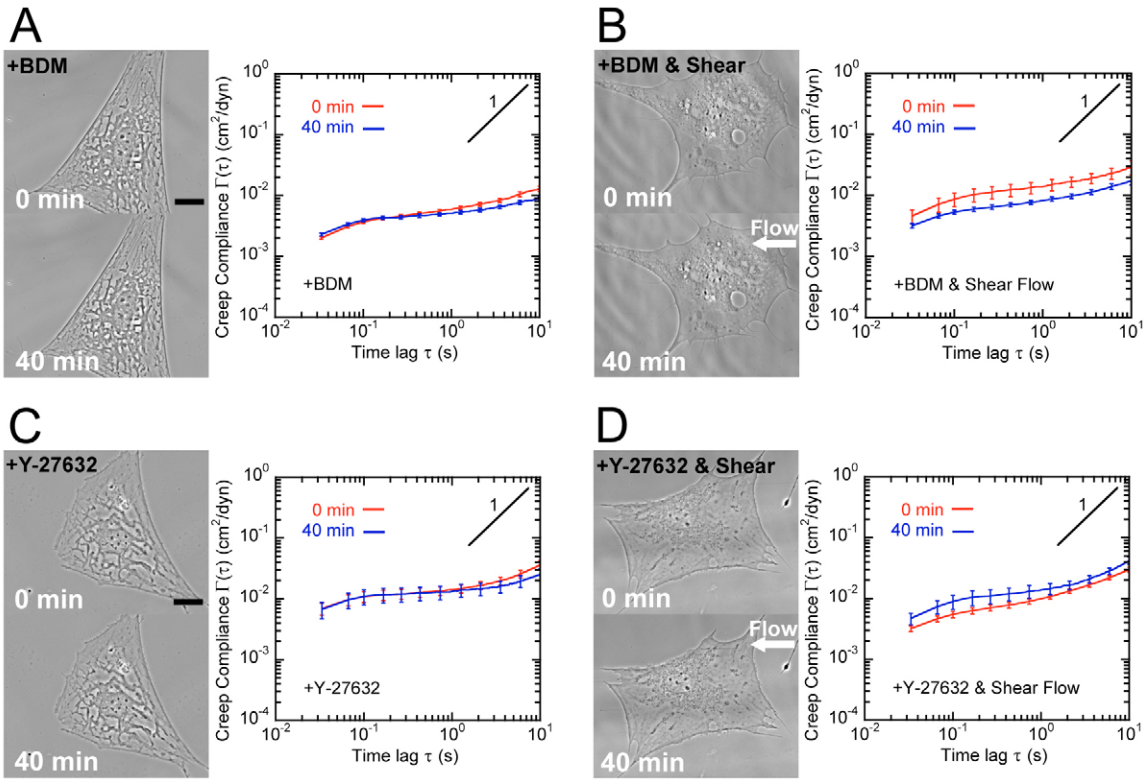

Fig. 3. Inhibition of actomyosin interaction or Rho-kinase diminishes the mechanical response of cells to shear flow. Cells were pretreated with BDM (20 mM) for 30 minutes to inhibit actomyosin interactions, and were either left unsheared (A) or sheared (B) for 40 minutes. Phase-contrast micrographs show minor changes in cell area and shape. Bar, 20 μm. Mean cellular compliances of unsheared fibroblasts (n=3) were similar after 40 minutes of BDM treatment. BDM treatment and shear flow caused fibroblasts to stiffen, but considerably less compared with control conditions, as shown by mean cellular compliances of sheared fibroblasts (n=4). Cells were also pretreated with specific Rho-kinase inhibitor Y-27632 (30 μM) for 30 minutes and were either left unsheared (C) or sheared (D) for 40 minutes. Phase-contrast micrographs show minor changes in cell area and shape. Bar, 20 μm. Mean cellular compliances of unsheared fibroblasts (n=3) were similar after 40 minutes of drug treatment. However, mean cellular compliances of sheared fibroblasts (n=4) show that cells did not stiffen in response to shear flow, and even became softer. All values represent mean ± s.e.m.

Rho-kinase inhibition abrogates shear-induced cytoplasmic stiffening

To further investigate the molecular basis of shear-induced cytoplasmic stiffening, we pretreated the cells with Y-27632, a highly specific inhibitor of p160ROCK (Kimura et al., 1996; Leung et al., 1996; Leung et al., 1995). Rho-kinase plays a key role in the regulation of actomyosin contractility through the inhibition of myosin light chain phosphatases and the phosphorylation of the myosin light chain (Burridge and Chrzanowska-Wodnicka, 1996; Kimura et al., 1996). Rho-kinase has also been shown to regulate actin filament reorganization by phosphorylation of LIM kinase (Ohashi et al., 2000; Sumi et al., 2001).

In unsheared cells, Y-27632 treatment caused minor cytoplasmic stiffening (Fig. 2B and Fig. 3C, n=3), possibly because of Y-27632-induced Rac activation (Nobes and Hall, 1999; Rottner et al., 1999). In sheared cells, Y-27632 completely abrogated shear-induced stiffening and even caused softening of the cytoplasm compared with Y-27632-treated unsheared cells (Fig. 3D, n=4), but not beyond that of cells before Y-27632 treatment (data not shown). Immunofluorescence revealed that sheared cells treated with Y-27632 showed a thick actin rim at the cell periphery and some F-actin in the perinuclear region – an actin filament architecture similar to that observed in unsheared control cells (Fig. 4A). Taken together, we conclude that the loss of Rho-kinase-mediated contractility renders the cytoskeleton unable to respond to external mechanical stimuli.

Discussion

Here we develop a new method of nanoparticle injection to probe for the first time the micromechanical response of the cytoplasm of adherent cells subjected to shear fluid flows by probing the random displacements of fluorescent nanoparticles embedded in the cytoplasm. Whether cells change the micromechanical properties of their cytoplasm in response to shear was previously unknown. Particle tracking and nanorheological analysis reveal that adherent fibroblasts respond to shear stresses by strengthening their cytoplasm. The shear viscosity of the cytoplasm of sheared cells increases 25-fold, which from a rheological standpoint would be akin to ketchup turning into peanut butter at room temperature. Shear-induced stiffening is diminished by reducing actomyosin interactions and completely abrogated following Rho-kinase inhibition, which indicates that actin-based contractility is a major contributor to the micromechanical response of cells to shear fluid flows.

These results suggest that when a quiescent cell without a

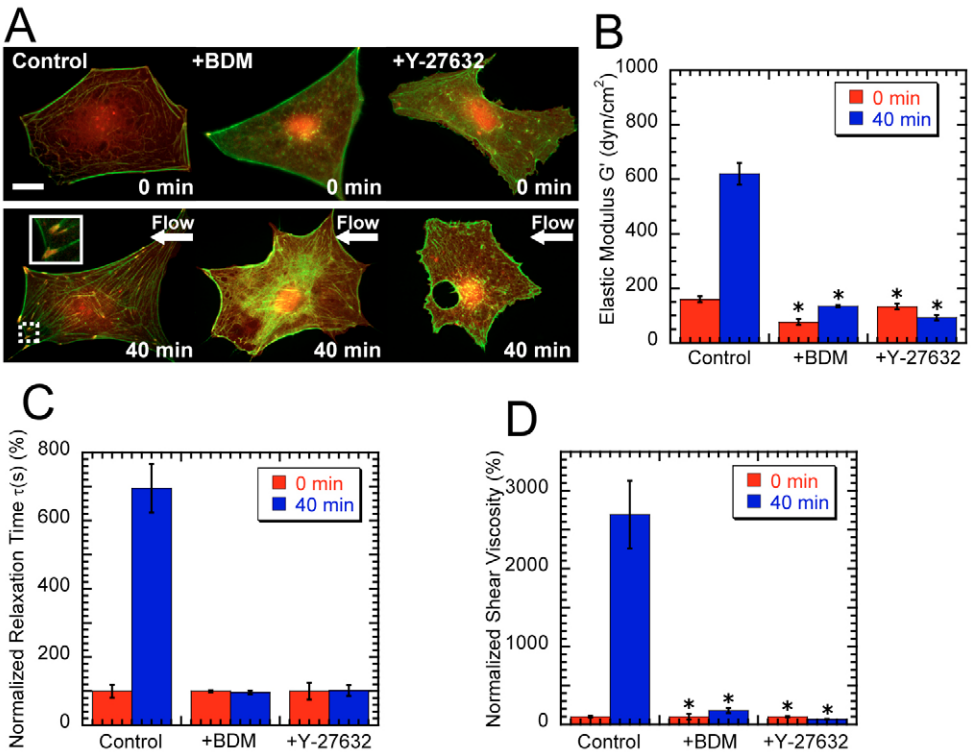

Fig. 4. Contractility and stress fiber/focal adhesion formation are needed for micromechanical response of cells to shear flow. (A) Immunofluorescence of actin (green) and vinculin (red) of unsheared (top) and sheared (bottom) Swiss 3T3 fibroblasts. Control fibroblasts exhibit extended stress fibers and large focal adhesions (Inset, bottom). The formation of these cytoskeleton structures was abrogated after cell treatment with inhibitors BDM (middle) or Y-27632 (right). Bar, 20 μm. (B) Comparison of plateau elastic moduli. Only untreated cells exhibited a significant increase in elasticity when subjected to fluid shear stress. This stiffness increase is reduced with BDM treatment, whereas a slight decrease in elasticity is observed with Y-27632 treatment. (C) Relaxation times of the cytoskeleton for each condition, which were normalized by each respective initial (unsheared) value. (D) Intracellular shear viscosity values for each condition, which were normalized by the initial value of the shear viscosity of unsheared cells. For (B) and (D), one-way ANOVA tests yielded $P<0.0001$; stars denote P values from two-tailed t-tests within conditions (see Materials and Methods). All values represent mean ± s.e.m.

well-established actin cytoskeleton (a serum-starved cell) is subjected to shear stresses, one of its first orders of action is to prevent its detachment from the substratum by greatly stiffening its cytoplasm through enhanced actin assembly and Rho-kinase-mediated cytoskeletal contractility. By contrast, a well-adherent cell with an organized, structured actin cytoskeleton (a cell in serum) can engage its microtubule network to polarize (Lee et al., 2005).

When developing an earlier version of the present assay, we verified that the presence of the probe nanoparticles in the cytoplasm – or even within the nucleus (Kole et al., 2004a; Tseng et al., 2004) – does not measurably affect normal cell function, including cell shape, cell growth, cell adhesion and cytoskeleton organization (Kole et al., 2004b). Moreover, the presence of the nanoparticles does not affect the global rheology of materials (Mason et al., 1997). However, ballistic injection transforms the particle-tracking rheology into a high-throughput biophysical method, while preserving single-cell resolution, and allows for the first time to probe cells in complex microenvironments, such as cells subjected to fluid flows.

Biochemical and biophysical stimuli lead to similar actin reorganizations, but different mechanical outcomes

Despite enhanced actin assembly and the appearance of stress fibers caused by fluid shear stress, the observed sustained dramatic increase in cytoplasmic stiffness was not expected a priori. Indeed, our previous study (Kole et al., 2004a) shows that the cytoplasm of serum-starved Swiss 3T3 fibroblasts stiffens only transiently upon LPA treatment, reaching much lower maxima of viscosity and elasticity, despite the fact that LPA induces the formation of long-lived contractile stress fibers that persist even after Rho activation subsides. Together these results suggest that biochemical (i.e. LPA) and biophysical stimuli (i.e. fluid shear stress) may elicit the formation of similar cytoskeleton architectures, but their micromechanical behaviors, as revealed by our functional BIN assay, are quantitatively different. This could be partly due to subtle differences in cytoskeleton organizations, which may not be readily detected by microscopy owing to limited resolution (Svitkina and Borisy, 1998). These changes may also be due to enhanced crosslinking among actin filaments, as demonstrated in reconstituted actin networks where minute variations in the concentration of F-actin crosslinking/bundling proteins can change their mechanical properties dramatically. For instance, the presence of the F-actin-crosslinking protein α-actinin at a molar ratio of 1:50 induces a 15-fold increase in network elasticity, even though this low α-actinin concentration largely preserves the spontaneous orthogonal

organization of actin filaments (Tseng et al., 2001; Tseng and Wirtz, 2001). This is due to the fact that a slight reduction in the relative motion of filaments in an entangled network caused by contractility or enhanced crosslinking can lead to vast increases in elasticity and viscosity.

Shear-induced cytoplasmic stiffening and the Rho/Rho-kinase transduction pathway

Our results, summarized in Fig. 5, suggest that a cell under shear combines two mechanisms to resist shear and remain firmly attached to the substratum: reorganization of the actin filament network and actomyosin contractility, which ultimately result in increased intracellular stiffness. Color-coding in Fig. 5 represents the level of shear viscosity of the cytoplasm normalized by its value before shear stimulation of the cells. Unsheared cells exhibit the lowest level of cytoplasmic shear viscosity (Fig. 5A, top) whereas sheared cells exhibit the highest viscosity (Fig. 5A, bottom). Inhibition of Rho-kinase abrogates this phenomenon completely (Fig. 5A, right), indicating that it has a key role in regulating intracellular stiffening. When actomyosin interactions are weakened and actin assembly is unaffected, cells exhibit a cytoplasmic viscosity that is intermediate between those of sheared and unsheared cells (Fig. 5A, left) and similar to that of LPA-treated cells (Fig. 5B). As BDM does not significantly affect actin filament assembly (Riveline et al., 2001; Wojciak-Stothard et al., 1998; Zhong et al., 1998), the intermediate cytoplasmic stiffening may be caused by shear-induced actin polymerization (Fig. 4A, middle), itself caused by the uninhibited activity of mDia (Ridley, 2001; Riveline et al., 2001; Tsuji et al., 2002; Watanabe et al., 1999) or LIM kinases (Ohashi et al., 2000; Sumi et al., 2001), both downstream effectors of Rho. Moreover, BDM is known to be a relatively weak inhibitor, which may allow residual actomyosin interactions (Fenteany and Zhu, 2003). Taken together, our results indicate that BIN does not merely confirm or quantify stress-fiber formation, but functionally distinguishes between similar actin-structure formations.

Differential micromechanical responses of cells subjected to LPA and shear flow

The difference between the sustained micromechanical response of cells to a mechanical stimulus (i.e. fluid shear stress) and their transient mechanical response to a chemical stimulus (i.e. LPA) (Fig. 5B) may be analogous to that between twitch and tetanus responses in muscle cells (Fig. 5C). When a biochemical stimulus is presented (i.e. LPA), a transient increase/decrease in cellular viscoelasticity occurs, analogous to a muscle twitch when a short-lived muscle input results in a rapid contraction followed by rapid relaxation. By contrast, when a sustained mechanical stimulus is presented, there is insufficient time to relax and therefore long-lived stiffening of

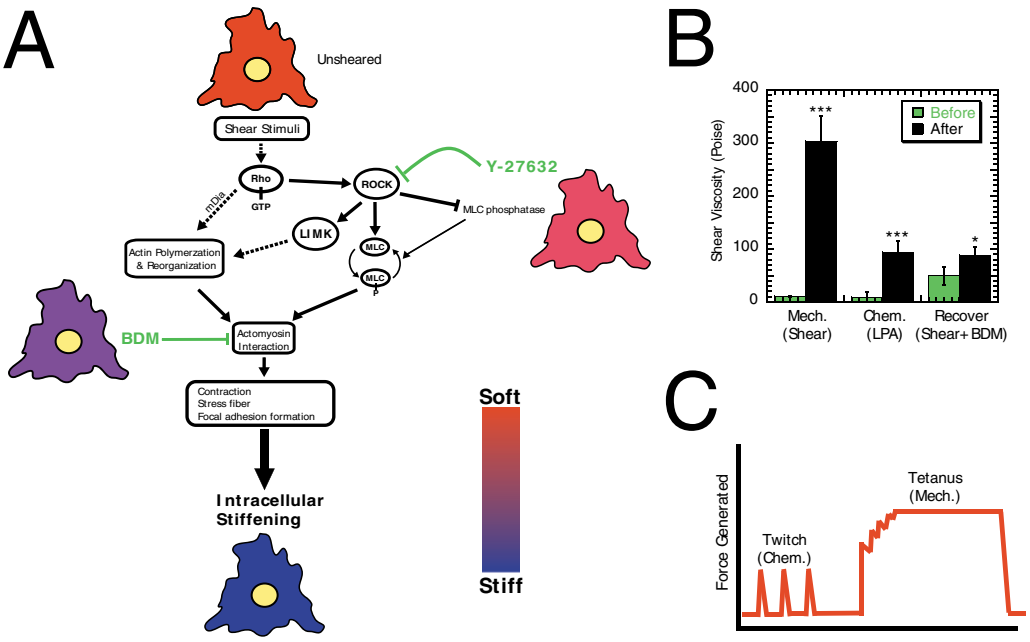

Fig. 5. Proposed signaling pathway describing the mechanical response of cytoplasm in cells subjected to shear flow. (A) Color-coded (see gradient legend bar) cell for each condition indicates changes in intracellular viscoelasticity with respect to unsheared conditions. Upon application of mechanical shear flow, activation of Rho causes the downstream activation of ROCK (ROK/Rho-kinase), LIM kinases, and mDia. Such activation results in (1) increased F-actin formation; (2) actomyosin contractility; (3) focal adhesion formation, and ultimately, significant intracellular cytoplasmic stiffening of Swiss 3T3 fibroblasts. Drug treatment experiments are shown in green. (B) Comparison of chemical and mechanical stimulation on intracellular mechanics. Biomechanical stimulus (shear flow) causes a sustained dramatic stiffening response whereas a biochemical stimulus (LPA) causes a transient intermediate stiffening response. Such an intermediate response is recovered in mechanical stimulation when actomyosin interactions are inhibited. One-way ANOVA test of shear data and previous LPA treatment data (Kole et al., 2004a) yielded $P<0.0001$. Stars denote P values from two-tailed t-tests within conditions (see Materials and Methods). (C) Illustration of twitch phenomenon in muscle cells versus sustained tetanus that occurs when there is insufficient time for relaxation, which is analogous to the difference in intracellular mechanics measured in biochemical versus biomechanical-stimulated cells.

the cytoplasm occurs, analogous to a sustained tetanus contraction (Fig. 5C). Such dramatic stiffening may not subside, as serum-starved cells exhibit no ordered cytoskeletal structure compared with serum-treated cells, and as the cells initially adapt their intracellular mechanics to shear flow and are continually being subjected to it, there would be no reason to soften until such stimuli is ceased. Transient activation/inactivation of Rho, followed by subsequent activation of Rac/Cdc42, have been shown to occur within 30 minutes in cells subjected to shear flow (Tzima et al., 2002; Tzima et al., 2001; Tzima et al., 2003). These changes in Rho GTPase activity have been shown to cause feedback formation of focal complexes to focal adhesions and vice versa (Rottner et al., 1999). Such feedback loops could be the cause of such a dramatic increase in cellular stiffness and should be further investigated using our BIN assay. In addition, intracellular micromechanical changes in response to varying duration and pattern of flow (e.g. pulsatile flows) would also be of interest.

In conclusion, our results reveal that adherent cells resist shear stresses to maintain adhesion to the substratum by strengthening their cytoplasm and identify Rho-kinase as a key regulator in the mechanotransduction pathway that controls cytoskeleton mechanics in cells subjected to shear stress. The high-throughput BIN assay developed here can now be used as a functional assay for many different applications, including identifying other regulators of the mechanical response of cells under shear stress, both upstream and downstream of RhoA/Rho-kinase. Our BIN assay could be readily applied to other systems where micromechanical information would be useful, such as understanding cellular motility in cancer metastasis or angiogenesis (Paszek et al., 2005; Zahir et al., 2003).

Materials and Methods

Materials and reagents

Thirty-five-mm glass bottom dishes (Matek, Ashland, MA) and 35-mm circle coverslips (VWR, West Chester, PA), used for shear flow experiments, were coated with 20 μg/ml fibronectin (Calbiochem, San Diego, CA), as described previously (Lee et al., 2005). Inhibitor drugs BDM and Y-27632 (Calbiochem) were both diluted with DMEM buffered with 25 mM HEPES (Invitrogen, Carlsbad, CA) to concentrations of 20 mM and 30 μM, respectively.

Cell culture and immunofluorescence

Swiss 3T3 fibroblasts (ATCC, Manassas, VA) were cultured in DMEM supplemented with 10% bovine calf serum (BCS, ATCC), 100 U penicillin and 100 μg streptomycin (Sigma, St Louis, MO) and maintained at 37°C in a humidified, 5% CO_2 environment. Cells were passaged every 3-4 days and seeded (approximately 1×10^4 cells/ml) onto 10-cm cell culture dishes (Corning, Corning, NY) in preparation for ballistic particle injection. Post injection, cells were plated using DMEM supplemented with 5% BCS (with 100 U penicillin and 100 μg streptomycin) on dishes prepared above. Culture medium was replaced the next day with serum-free DMEM supplemented with 100 U penicillin and 100 μg streptomycin. Cells were serum-starved for 48 hours prior to all experiments. Immunostaining of cells was conducted using Alex Fluor 350-labeled anti-vinculin (Sigma) and Alex Fluor 488 phalloidin (Invitrogen), as described previously (Lee et al., 2005). Fluorescent images were collected using an Orca II CCD camera (Hammamatsu, Bridgewater, NJ) mounted on a Nikon TE2000E microscope with a 60× Plan Fluor lens controlled by Metavue software.

Rheological definitions

Here we define the rheological terms used in the paper – including viscosity, elasticity, creep compliance, and relaxation time – for the non-specialist (see Heidemann and Wirtz, 2004). For an ideal elastic material (such as rubber), the extent of deformation of the material is directly related to the applied force. This characteristic behavior of solids is caused by strong interactions among neighboring molecules. One molecule cannot be moved without neighboring molecules also responding. Solids and ideal elastics respond instantaneously to forces and deformations. They also store energy: when an applied force is removed, the elastic recoils without any energy loss. Solids are characterized by an elastic modulus or elasticity (also called stiffness or stretchiness). For ideal liquids (such as water, glycerol or honey), the force is directly related to the rate of deformation. Here each molecule is able to move freely and independently of its neighboring molecules in response to applied forces. Liquids do not store energy when subjected to deformations, but continuously dissipate energy. Viscous liquids are characterized by a shear viscosity. The cytoskeleton, which dominates the rheological behavior of the cytoplasm, is composed of filamentous structures that render the cytoplasm both elastic and viscous, i.e. viscoelastic. Entanglements between polymers inhibit the free movement of these polymers in the network that they form. The rheological response of polymers that are entangled (and not crosslinked) depends highly on the speed of the applied force or deformation – more elastic in response to rapid interventions, but less stiff and more viscous in response to slower interventions. If polymer chains are crosslinked, then they show only an elastic solid-like behavior. The stiffness of crosslinked polymers does not depend on the rate of deformation and they primarily behave elastically. The creep compliance, also reported in this paper, measures the extent of deformation of a material when subjected to a mechanical stress. For a viscous liquid, the creep compliance or deformation caused by an applied stress will increase linearly with time. For an elastic solid, the compliance increases immediately after application of the stress, but remains subsequently unchanged. For a visco-elastic material, the time-dependent compliance is intermediate between those of a viscous liquid and an elastic solid, and therefore increases more slowly than linearly with time. For an entangled cytoskeletal polymer network, the relaxation time is the averaged time it takes for a polymer to disentangle itself from its surrounding polymers. The relaxation time increases with the lifetime of the crosslinks formed between cytoskeletal polymers. For a permanently crosslinked polymer network, the relaxation time becomes infinite.

Shear flow assay

A parallel-plate flow chamber (GlycoTech, Rockville, MD) was used to apply fluid shear stress to Swiss 3T3 fibroblasts, as described previously (Lee et al., 2005). Briefly, cells were subjected to a wall shear stress of 9.4 dynes/cm^2 for 40 minutes using a flow of serum-free DMEM buffered with 25 mM HEPES. Particle-tracking movies were recorded before and after shear stimulus. We note that while measurements were made post stimulus, no more than 1 minute occurred between cessation of stimulus and complete recording of particle tracking movies. For experiments with inhibitors, cells were pretreated with either BDM or Y-27632 at specified concentrations for 30 minutes prior to shear stimulus. Drug concentrations were maintained in flow medium to prevent recovery from drug inhibition. Pretreated cells were also left unsheared for 40 minutes to ensure that the drugs did not significantly alter cell mechanics (Fig. 3A,C).

Shear-induced cell polarization assay

Potential shear-induced cell polarization was assessed using the assay described previously (Lee et al., 2005). Briefly, sheared cells were fixed with 2% paraformaldehyde for 1 hour, permeabilized with 0.1% Triton X-100 for 10 minutes, blocked using 10% BCS in PBS for 20 minutes and then were treated with α-tubulin mAb (Oncogene) at a 1:20 dilution. Next, cells were incubated in Alexa Fluor 568 goat anti-mouse antibody at 1:40 and 300 nM of DAPI for 1 hour (Invitrogen) to visualize microtubules and nuclear DNA, respectively. MTOC location was determined by first overlaying Alexa Fluor 568 and DAPI fluorescence images using Metamorph. The nucleus was divided into two regions – one in the direction and one in the opposing direction of flow – to determine the location of the MTOC with respect to the division. Approximately 70-80 cells were assessed for each condition.

Ballistic particle injection, particle tracking, and cytoplasmic rheology

Fibroblasts plated on 10-cm cell culture dishes were subjected to ballistic injection of 100-nm-diameter fluorescent nanoparticles (Invitrogen) using a Biolistic PDS-1000/HE particle-delivery system (Bio-Rad, Richmond, CA). Nanoparticles were placed on macrocarriers and allowed to dry for 2 hours. 2200 psi rupture disks were used in conjunction with a hepta adapter. Problems could arise when nanoparticles do not penetrate the cytoplasm directly upon impact, which may then be engulfed by the cell through endocytosis and undergo microtubule-mediated directed motion (Tseng et al., 2002). We circumvented this problem by thoroughly and repeatedly washing the cells with fresh medium right after ballistic bombardment. We found that none of the probed nanoparticles underwent directed motion.

Using a silicon-intensifier target (SIT) camera (VE-100 Dage-MTI, Michigan City, IN) mounted on a Nikon TE2000E epifluorescence microscope and a 60× Plan Fluor oil-immersion lens (NA 1.4, Nikon, Melville, NY), movies capturing the Brownian motion of the ballistically injected nanoparticles were collected at 30 frames/second using Metavue software (Universal Imaging, West Chester, PA). Movie analysis was conducted first using Metamorph software (Universal Imaging) and then using a custom software was used to obtain rheological parameters describing the viscoelastic properties of the cytoplasm (Kole et al., 2004a), including elastic and viscous moduli, shear viscosity, and creep compliance. The

random displacements of the nanoparticles centroids were tracked for 20 seconds at a rate of 30 frames/second. At least 120 different nanoparticles were tracked per condition. The time-averaged mean squared displacement (MSD), $\langle \Delta r^2(\tau) \rangle = \langle [x(t + \tau) - x(t)]^2 + [x(t + \tau) - y(t)]^2 \rangle$, where τ is the time scale and t is the elapsed time, was calculated from the trajectory of the light intensity-weighted centroid of each microsphere. Previous studies have already examined the effects of size and surface chemistry of the nanoparticles in cells (Kole et al., 2005; Panorchan et al., 2004; Tseng et al., 2002). It is important to note that each movie is much shorter than that the characteristic time scales of cell migration. We assumed that the time-averaged movements of the nanoparticles in the x, y, and z directions were identical. To test this assumption, we verified and found that the MSDs of individual nanoparticles in the x and y directions were identical, $\langle \Delta x^2(\tau) \rangle = \langle \Delta y^2(\tau) \rangle$ so that $\langle \Delta r^2(\tau) \rangle = 2\langle \Delta x^2(\tau) \rangle = 2\langle \Delta y^2(\tau) \rangle$ (Haber et al., 2000). This suggests that, for the short times of movie capture, the cytoplasm around each nanosphere can be considered to be isotropic, i.e. it has the same physical properties in the x and y directions, and therefore the z direction.

We note that there is a fundamental difference between the spatial resolution on size and spatial resolution on displacements obtained with the same light microscope. The size resolution for a light microscope is about 200 nm. We do not measure the size of objects, but measure their displacements. By tracking the centroid displacements of the nanoparticles, we can reach a sub-pixel spatial resolution on the displacements of 10 nm. Indeed a small displacement of the nanoparticle will induce a displacement of the centroid of the light-intensity profile of the diffraction-limited image of each nanoparticle, which is readily detected with sub-pixel resolution. We measured directly the displacement resolution of our tracking method by tethering (using crazy glue) the same type of nanoparticles that we used in the live-cell experiments to a glass coverslip and probed the apparent displacements of those nanoparticles. The square root of the MSDs of these 'immobile' nanoparticles is the real displacement resolution of our microscopy/particle-tracking system, which is 10 nm.

The MSD of each probe nanosphere is directly related to the local creep compliance of the cytoplasm, $\Gamma(\tau)$, as (Xu et al., 1998):

$$\Gamma(\tau) = \frac{3\pi a}{2k_B T} \langle \Delta r^2(\tau) \rangle .$$

The creep compliance (expressed in units of cm^2/dyn, the inverse of a modulus) describes the local deformation of the cytoplasm induced by the forces acting on the surface of the nanoparticles and created by the thermally excited displacements of the nanoparticles. If the cytoplasm around a nanosphere behaves like a liquid (e.g. glycerol), then the creep compliance increases continuously and linearly with time, with a slope that is inversely proportional to the shear viscosity, $\Gamma(\tau) = \tau/\eta$. If the cytoplasm behaves locally like a solid gel, then the creep compliance is a constant with a value inversely proportional to the elasticity of the gel, $\Gamma(\tau) = 1/G_0$. The local frequency-dependent viscoelastic parameters of the cytoplasm, $G'(\omega)$ and $G''(\omega)$ (both expressed in units of dyn/cm^2, a force per unit area), are computed straightforwardly from the MSD, as described previously (Kole et al., 2005; Tseng et al., 2002). The elastic modulus, G', and viscous modulus, G'', describe the propensity of a complex fluid to resist elastically and to flow under mechanical stress, respectively. A filamentous structure, such as a reconstituted F-actin network or the cytoplasm of cells, behaves like a solid elastic gel at high rates of shear (high frequencies ω), when filaments do not have the time to relax during shear, and like a liquid at low rates of shear. The crossover rate of shear between these two rheological behaviors [the frequency for which $G'(\omega)=G''(\omega)$, Fig. 2C] corresponds to the inverse of the relaxation time. The mean shear viscosity of the cytoplasm can be approximated as the product of the mean relaxation time and the mean plateau value of the elastic modulus of the cytoplasm. We note that the measurements of the bulk rheological properties of standard fluids (e.g. glycerol, DNA or F-actin) obtained by a cone-and-plate rheometer compare quantitatively with those obtained using the particle tracking approach used here (Mason et al., 1997; Xu et al., 1998).

Statistical analysis

Mean values, standard error of measurement (s.e.m.), and statistical analysis for creep compliance, elastic modulus, relaxation time, and shear viscosity were calculated using Graphpad Prism (Graphpad Software, San Diego, CA) and plotted using Kaleidagraph (Kaleidagraph, Reading, PA) for these rheological parameters. Two-tailed unpaired *t*-tests were conducted within control and drug-treated conditions to determine significance of change caused by shear stimuli. Significance was indicated on graphs using ***P<0.001, **P<0.01 and *P<0.05. One-way ANOVA tests were also conducted across conditions for elastic moduli and shear viscosity values, and corresponding P values are reported.

This work was supported by a NIH grant (R01 GM075305-01) (to D.W.) and a NASA grant (NAG9-1563) (to D.W. and Y.T.). J.S.H.L. was supported by a NASA graduate training grant (NNG04G054H).

References

Burridge, K. and Chrzanowska-Wodnicka, M. (1996). Focal adhesions, contractility, and signaling. *Annu. Rev. Cell Dev. Biol.* **12**, 463-518.

Danowski, B. A. (1998). Microtubule dynamics in serum-starved and serum-stimulated Swiss 3T3 mouse fibroblasts: implications for the relationship between serum-induced contractility and microtubules. *Cell Motil. Cytoskeleton* **40**, 1-12.

Evans, E., Ritchie, K. and Merkel, R. (1995). Sensitive force technique to probe molecular adhesion and structural linkages at biological interfaces. *Biophys. J.* **68**, 2580-2587.

Fenteany, G. and Zhu, S. (2003). Small-molecule inhibitors of actin dynamics and cell motility. *Curr. Top. Med. Chem.* **3**, 593-616.

Gimbrone, M. A., Jr (1999). Vascular endothelium, hemodynamic forces, and atherogenesis. *Am. J. Pathol.* **155**, 1-5.

Girard, P. R. and Nerem, R. M. (1995). Shear stress modulates endothelial cell morphology and F-actin organization through the regulation of focal adhesion-associated proteins. *J. Cell Physiol.* **163**, 179-193.

Haber, C., Alom-Ruiz, S. and Wirtz, D. (2000). Shape anisotropy of a single random-walk polymer. *Proc. Natl. Acad. Sci. USA* **97**, 10792-10795.

Hall, A. (1998). Rho GTPases and the actin cytoskeleton. *Science* **279**, 509-514.

Heidemann, S. R. and Wirtz, D. (2004). Towards a regional approach to cell mechanics. *Trends Cell Biol.* **14**, 160-166.

Hoh, J. H. and Schoenenberger, C. A. (1994). Surface morphology and mechanical properties of MDCK monolayers by atomic force microscopy. *J. Cell Sci.* **107**, 1105-1114.

Ji, J. Y., Jing, H. and Diamond, S. L. (2003). Shear stress causes nuclear localization of endothelial glucocorticoid receptor and expression from the GRE promoter. *Circ. Res.* **92**, 279-285.

Kimura, K., Ito, M., Amano, M., Chihara, K., Fukata, Y., Nakafuku, M., Yamamori, B., Feng, J., Nakano, T., Okawa, K. et al. (1996). Regulation of myosin phosphatase by Rho and Rho-associated kinase (Rho-kinase). *Science* **273**, 245-248.

Kole, T. P., Tseng, Y., Huang, L., Katz, J. L. and Wirtz, D. (2004a). Rho kinase regulates the intracellular micromechanical response of adherent cells to rho activation. *Mol. Biol. Cell* **15**, 3475-3484.

Kole, T. P., Tseng, Y. and Wirtz, D. (2004b). Intracellular microrheology as a tool for the measurement of the local mechanical properties of live cells. *Methods Cell Biol.* **78**, 45-64.

Kole, T. P., Tseng, Y., Jiang, I., Katz, J. L. and Wirtz, D. (2005). Intracellular mechanics of migrating fibroblasts. *Mol. Biol. Cell* **16**, 328-338.

Langille, B. L., Graham, J. J., Kim, D. and Gotlieb, A. I. (1991). Dynamics of shear-induced redistribution of F-actin in endothelial cells in vivo. *Arterioscler. Thromb.* **11**, 1814-1820.

Lee, J. S., Chang, M. I., Tseng, Y. and Wirtz, D. (2005). Cdc42 mediates nucleus movement and MTOC polarization in Swiss 3T3 fibroblasts under mechanical shear stress. *Mol. Biol. Cell* **16**, 871-880.

Leung, T., Manser, E., Tan, L. and Lim, L. (1995). A novel serine/threonine kinase binding the Ras-related RhoA GTPase which translocates the kinase to peripheral membranes. *J. Biol. Chem.* **270**, 29051-29054.

Leung, T., Chen, X. Q., Manser, E. and Lim, L. (1996). The p160 RhoA-binding kinase ROK alpha is a member of a kinase family and is involved in the reorganization of the cytoskeleton. *Mol. Cell. Biol.* **16**, 5313-5327.

Malek, A. M. and Izumo, S. (1996). Mechanism of endothelial cell shape change and cytoskeletal remodeling in response to fluid shear stress. *J. Cell Sci.* **109**, 713-726.

Mason, T. G., Ganesan, K., van Zanten, J. V., Wirtz, D. and Kuo, S. C. (1997). Particle-tracking microrheology of complex fluids. *Phys. Rev. Lett.* **79**, 3282-3285.

McKillop, D. F., Fortune, N. S., Ranatunga, K. W. and Geeves, M. A. (1994). The influence of 2,3-butanedione 2-monoxime (BDM) on the interaction between actin and myosin in solution and in skinned muscle fibres. *J. Muscle Res. Cell Motil.* **15**, 309-318.

Ng, C. P. and Swartz, M. A. (2003). Fibroblast alignment under interstitial fluid flow using a novel 3-D tissue culture model. *Am J. Physiol. Heart Circ. Physiol.* **284**, H1771-H1777.

Ng, C. P., Hinz, B. and Swartz, M. A. (2005). Interstitial fluid flow induces myofibroblast differentiation and collagen alignment in vitro. *J. Cell Sci.* **118**, 4731-4739.

Nobes, C. D. and Hall, A. (1995). Rho, rac, and cdc42 GTPases regulate the assembly of multimolecular focal complexes associated with actin stress fibers, lamellipodia, and filopodia. *Cell* **81**, 53-62.

Nobes, C. D. and Hall, A. (1999). Rho GTPases control polarity, protrusion, and adhesion during cell movement. *J. Cell Biol.* **144**, 1235-1244.

Ohashi, K., Nagata, K., Maekawa, M., Ishizaki, T., Narumiya, S. and Mizuno, K. (2000). Rho-associated kinase ROCK activates LIM-kinase 1 by phosphorylation at threonine 508 within the activation loop. *J. Biol. Chem.* **275**, 3577-3582.

Palazzo, A. F., Joseph, H. L., Chen, Y. J., Dujardin, D. L., Alberts, A. S., Pfister, K. K., Vallee, R. B. and Gundersen, G. G. (2001). Cdc42, dynein, and dynactin regulate MTOC reorientation independent of Rho-regulated microtubule stabilization. *Curr. Biol.* **11**, 1536-1541.

Panorchan, P., Tseng, Y. and Wirtz, D. (2004). Structure-function relationship of biological gels revealed by multiple particle tracking and differential interference contrast microscopy: The case of human lamin networks. *Phys Rev. E* **70**, 041906.

Paszek, M. J., Zahir, N., Johnson, K. R., Lakins, J. N., Rozenberg, G. I., Gefen, A., Reinhart-King, C. A., Margulies, S. S., Dembo, M., Boettiger, D. et al. (2005). Tensional homeostasis and the malignant phenotype. *Cancer Cell* **8**, 241-254.

Poli, A., Scott, D., Bertin, K., Miserocchi, G., Mason, R. M. and Levick, J. R. (2001).

Influence of actin cytoskeleton on intra-articular and interstitial fluid pressures in synovial joints. *Microvasc. Res.* **62**, 293-305.

Ridley, A. J. (2001). Rho family proteins: coordinating cell responses. *Trends Cell Biol.* **11**, 471-477.

Ridley, A. J. and Hall, A. (1992). The small GTP-binding protein rho regulates the assembly of focal adhesions and actin stress fibers in response to growth factors. *Cell* **70**, 389-399.

Ridley, A. J., Paterson, H. F., Johnston, C. L., Diekmann, D. and Hall, A. (1992). The small GTP-binding protein rac regulates growth factor-induced membrane ruffling. *Cell* **70**, 401-410.

Riveline, D., Zamir, E., Balaban, N. Q., Schwarz, U. S., Ishizaki, T., Narumiya, S., Kam, Z., Geiger, B. and Bershadsky, A. D. (2001). Focal contacts as mechanosensors: externally applied local mechanical force induces growth of focal contacts by an mDia1-dependent and ROCK-independent mechanism. *J. Cell Biol.* **153**, 1175-1186.

Rottner, K., Hall, A. and Small, J. V. (1999). Interplay between Rac and Rho in the control of substrate contact dynamics. *Curr. Biol.* **9**, 640-648.

Sumi, T., Matsumoto, K. and Nakamura, T. (2001). Specific activation of LIM kinase 2 via phosphorylation of threonine 505 by ROCK, a Rho-dependent protein kinase. *J. Biol. Chem.* **276**, 670-676.

Svitkina, T. M. and Borisy, G. G. (1998). Correlative light and electron microscopy of the cytoskeleton of cultured cells. *Methods Enzymol.* **298**, 570-592.

Thoumine, O. and Ott, A. (1997). Time scale dependent viscoelastic and contractile regimes in fibroblasts probed by microplate manipulation. *J. Cell Sci.* **110**, 2109-2116.

Tseng, Y. and Wirtz, D. (2001). Mechanics and multiple-particle tracking microheterogeneity of alpha-actinin-cross-linked actin filament networks. *Biophys. J.* **81**, 1643-1656.

Tseng, Y., Fedorov, E., McCaffery, J. M., Almo, S. C. and Wirtz, D. (2001). Micromechanics and ultrastructure of actin filament networks crosslinked by human fascin: a comparison with alpha-actinin. *J. Mol. Biol.* **310**, 351-366.

Tseng, Y., Kole, T. P. and Wirtz, D. (2002). Micromechanical mapping of live cells by multiple-particle-tracking microrheology. *Biophys. J.* **83**, 3162-3176.

Tseng, Y., Lee, J. S., Kole, T. P., Jiang, I. and Wirtz, D. (2004). Micro-organization and visco-elasticity of the interphase nucleus revealed by particle nanotracking. *J. Cell Sci.* **117**, 2159-2167.

Tsuji, T., Ishizaki, T., Okamoto, M., Higashida, C., Kimura, K., Furuyashiki, T., Arakawa, Y., Birge, R. B., Nakamoto, T., Hirai, H. et al. (2002). ROCK and mDia1 antagonize in Rho-dependent Rac activation in Swiss 3T3 fibroblasts. *J. Cell Biol.* **157**, 819-830.

Tzima, E., del Pozo, M. A., Shattil, S. J., Chien, S. and Schwartz, M. A. (2001). Activation of integrins in endothelial cells by fluid shear stress mediates Rho-dependent cytoskeletal alignment. *EMBO J.* **20**, 4639-4647.

Tzima, E., Del Pozo, M. A., Kiosses, W. B., Mohamed, S. A., Li, S., Chien, S. and Schwartz, M. A. (2002). Activation of Rac1 by shear stress in endothelial cells mediates both cytoskeletal reorganization and effects on gene expression. *EMBO J.* **21**, 6791-6800.

Tzima, E., Kiosses, W. B., del Pozo, M. A. and Schwartz, M. A. (2003). Localized cdc42 activation, detected using a novel assay, mediates microtubule organizing center positioning in endothelial cells in response to fluid shear stress. *J. Biol. Chem.* **278**, 31020-31023.

Wang, N., Butler, J. P. and Ingber, D. E. (1993). Mechanotransduction across the cell surface and through the cytoskeleton. *Science* **260**, 1124-1127.

Watanabe, N., Kato, T., Fujita, A., Ishizaki, T. and Narumiya, S. (1999). Cooperation between mDia1 and ROCK in Rho-induced actin reorganization. *Nat. Cell Biol.* **1**, 136-143.

Wojciak-Stothard, B. and Ridley, A. J. (2003). Shear stress-induced endothelial cell polarization is mediated by Rho and Rac but not Cdc42 or PI 3-kinases. *J. Cell Biol.* **161**, 429-439.

Wojciak-Stothard, B., Entwistle, A., Garg, R. and Ridley, A. J. (1998). Regulation of TNF-alpha-induced reorganization of the actin cytoskeleton and cell-cell junctions by Rho, Rac, and Cdc42 in human endothelial cells. *J. Cell. Physiol.* **176**, 150-165.

Xu, J., Viasnoff, V. and Wirtz, D. (1998). Compliance of actin filament networks measured by particle-tracking microrheology and diffusing wave spectroscopy. *Rheol. Acta* **37**, 387-398.

Zahir, N., Lakins, J. N., Russell, A., Ming, W., Chatterjee, C., Rozenberg, G. I., Marinkovich, M. P. and Weaver, V. M. (2003). Autocrine laminin-5 ligates alpha6beta4 integrin and activates RAC and NFkappaB to mediate anchorage-independent survival of mammary tumors. *J. Cell Biol.* **163**, 1397-1407.

Zheng, J., Lamoureux, P., Santiago, V., Dennerll, T., Buxbaum, R. E. and Heidemann, S. R. (1991). Tensile regulation of axonal elongation and initiation. *J. Neurosci.* **11**, 1117-1125.

Zhong, C., Chrzanowska-Wodnicka, M., Brown, J., Shaub, A., Belkin, A. M. and Burridge, K. (1998). Rho-mediated contractility exposes a cryptic site in fibronectin and induces fibronectin matrix assembly. *J. Cell Biol.* **141**, 539-551.